# Pentamodes

## Effect of unit cell topology on mechanical properties

Mohammadi, Kaivan; Shafia, Moein; Akbari, Javad; Hedayati, Reza

**DOI**
10.1016/j.rineng.2024.101982

**Publication date**
2024

**Document Version**
Final published version

**Published in**
Results in Engineering

**Citation (APA)**
Mohammadi, K., Shafia, M., Akbari, J., & Hedayati, R. (2024). Pentamodes: Effect of unit cell topology on mechanical properties. *Results in Engineering*, *22*, Article 101982. https://doi.org/10.1016/j.rineng.2024.101982

Results in Engineering 22 (2024) 101982

Contents lists available at ScienceDirect

Results in Engineering

journal homepage: www.sciencedirect.com/journal/results-in-engineering

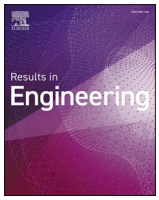

# Pentamodes: Effect of unit cell topology on mechanical properties

Kaivan Mohammadi [a], Moein Shafia [a], Javad Akbari [a], Reza Hedayati [b,*]

[a] Advanced Manufacturing Lab (AML), Department of Mechanical Engineering, Sharif University of Technology, Azadi Avenue, 11365-11155, Tehran, Iran
[b] Aerospace Materials and Structures Department, Faculty of Aerospace Engineering, Delft University of Technology (TU Delft), Kluyverweg 1, 2629, HS Delft, the Netherlands

ARTICLE INFO

*Keywords:*
Pentamodes
Metamaterials
Meta-fluids
3D printing

ABSTRACT

Pentamodes (first conceived theoretically by Milton and Cherkaev) are a very interesting class of mechanical metamaterials that can be used as building blocks of structures withdecoupled bulk and shear moduli. The pentamodes usually are composed of double cone-shaped struts with the middle diameter being large and the end diameters being tiny (ideally approaching zero). The cubic diamond geometry was proposed by Milton and Cherkaev as a suitable geometry for the unit cell and has since been used in the majority of the works on pentamodes. In this work, we aim to evaluate the degree to which the base unit cell design contributes to high bulk to shear modulus ratio, also known as Figure Of Merit(FOM). In addition to the diamond unit cell, three other well-known unit cell types are considered, and the effect of small diameter size and the ratio of large-to-small diameter, α, on the FOM is evaluated. The results showed that regardless of the base unit cell shape, the FOM value is highly dependent on the $d$ (the smaller diameter size of double-cone) value, while its dependence on the $D$ (the greater diameter of double-cone) value is very weak. For $d/h \propto 0.05$ ($h$ representing the linkage length), figures of merit in the range of $10^3$ could be reached for all the studied topologies.

## 1. Introduction

Mechanical metamaterials are a new class of designer materials that exhibit elastic properties rarely found in nature [1–5]. Such rationally-designed materials include materials with negative Poisson's ratio (known as auxetics) [6–8], materials with negative stiffness [9,10], and pentamodes [11–13].

The inverse problem of finding a microstructure that can give the wanted mechanical properties is very difficult. This can be attributed to the fact that, unlike many other fields such as heat conduction, electric conduction, diffusion, etc., the underlying equations for mechanical response of continuum-mechanics equations are not form-invariant [14]. Direct lattice transformation approaches are simpler and easier to implement. Many efforts have been made toward design approaches to gain prescribed constitutive properties, the first of which can be attributed to the pentamode structures introduced theoretically by Milton and Cherkaev [15].

Pentamodes are metamaterials that, at least in theory, can be used as building blocks of materials with any arbitrarily chosen elastic properties in different directions. This has led to a very practical application of pentamode metamaterials where the bulk and shear moduli can be decoupled. In many use cases, pentamodes have very large bulk moduli compared to their shear moduli [16–18], leading to the use of the term "metafluids" for them [19]. Ideally, the 6 × 6 elasticity tensor of these materials has 5 ("penta") zero members, and only one member is non-zero [15,19]. The pentamodes usually are composed of double cone-shaped struts with the middle diameter being large and the end diameters being tiny (ideally approaching zero). A perfect pentamode metamaterial flows away with very small shear forces, and that's why, in practice, a small but "finite" shear modulus is needed. Therefore, in the majority of the previously manufactured pentamode metamaterials [16,19], the end diameters of the struts are small (but non-zero). Using numerical and experimental studies, Kadic et al. [17], Martin et al. [13], Schittny et al. [16], and Hedayati et al. [20] have shown that the smaller diameter of the double cones (in the vertices of the lattice structure) are the most determinant parameter in the mechanical properties of low-density pentamode metamaterials. There are other more recent works that have explored the change of struts cross-sections within the lattice structures with struts that are not cone-shaped [21,22].

Milton and Cherkaev [15] proposed a diamond unit cell for such a structure in which four linkages meet in equal angles at each vertex of the structure. They proposed this morphology in analogy with bimode

* Corresponding author.
*E-mail addresses:* r.hedayati@tudelft.nl, rezahedayati@gmail.com (R. Hedayati).

https://doi.org/10.1016/j.rineng.2024.101982
Received 8 October 2023; Received in revised form 20 February 2024; Accepted 4 March 2024
Available online 11 March 2024

metamaterials, which can only support a single stress in two-dimensional space. In their proposed design for bimode, three linkages met at a point. Therefore, they concluded that a natural way towards 3D extremal material (pentamodes) is to consider a unit cell shape where only four linkages meet at the vertices. The diamond geometry has since been used in majority of the works on pentamodes.

In this work, we aim to evaluate the degree to which the main unit cell design contributes to high bulk-to-shear modulus ratio (known as FOM). As shown in Fig. 1, in addition to the diamond unit cell, three other well-known unit cell designs are considered, and the effect of small diameter size and the ratio of large-to-small diameter ratio, $\alpha$, on the FOM is evaluated.

## 2. Materials and methods

Creality LD-002R LCD 3D printer with ESUN PLA resins (Polyurethane acrylate) was used to manufacture all the specimens with a layer height of 30 $\mu m$. The curing time was set to 7 s. The geometrical dimensions of $h = 4\ mm$, $D = 1200\ \mu m$, and $d = 400\ \mu m$ were used for all the manufactured specimens (Fig. 2). All the lattice structures were composed of $5 \times 5 \times 5$ unit cells in each direction. The dimensions of the lattice structures based on cube, truncated cube, truncated octahedron, and diamond unit cells were $21.42 \pm 0.45\ mm$, $49.72 \pm 0.37\ mm$, $57.83 \pm 0.15\ mm$, and $40.83 \pm 0.25\ mm$, respectively. The mechanical properties of the constituent polymer were obtained using dog-bone specimens according to ISO D638-14. The bulk material had an elastic modulus of $E_s = 0.51\ GPa$, yield strength of $\sigma_{ys} = 28.0\ MPa$, Poisson's ratio of $\nu_s = 0.4$, and density of $\rho_s = 1020\ kg/m^3$.

The compression experimental tests were performed using SANTAM STM-20 (Tehran, Iran) mechanical test bench under a displacement rate of 2.5 mm/min. Moreover, 20 kgf load cells were implemented to measure the load level in the truncated cube and truncated octahedron topologies, while 100 kgf load cells were used for measuring the forces in the cube topology. One of the crucial factors influencing the accuracy of the results is the load cell's capacity. Given the delicate nature of the manufactured samples and the anticipation of limited force-bearing capacity, a load cell with lower capacity has been opted for measuring the load level in the truncated cube and truncated octahedron topologies.

Based on the microscopic measurements performed on the manufactured specimens, numerical finite element (FE) models were constructed and solved in COMSOL Multiphysics package (Sweden). To discretize the models, approximately $\sim 10^7$ tetrahedral elements were employed. A mesh sensitivity analysis was conducted to ensure numerical convergence, resulting in optimum element sizes smaller than 14 μm at diameter $d$ and 110 μm at diameter $D$. The MUMPS static solver in COMSOL was utilized to solve the continuum mechanics equations. A linear elastic material model was implemented, adopting the mechanical properties of the constituent polymeric material that was obtained from standard tensile test. A uniform displacement of 1010 μm was applied to the top side of the lattice structure in ten incremental steps.

In the models constructed for uniaxial compressive loading (Table 1), all the nodes at the lowermost surface of the lattice structures were allowed to move in their plane only, and they were constrained in the

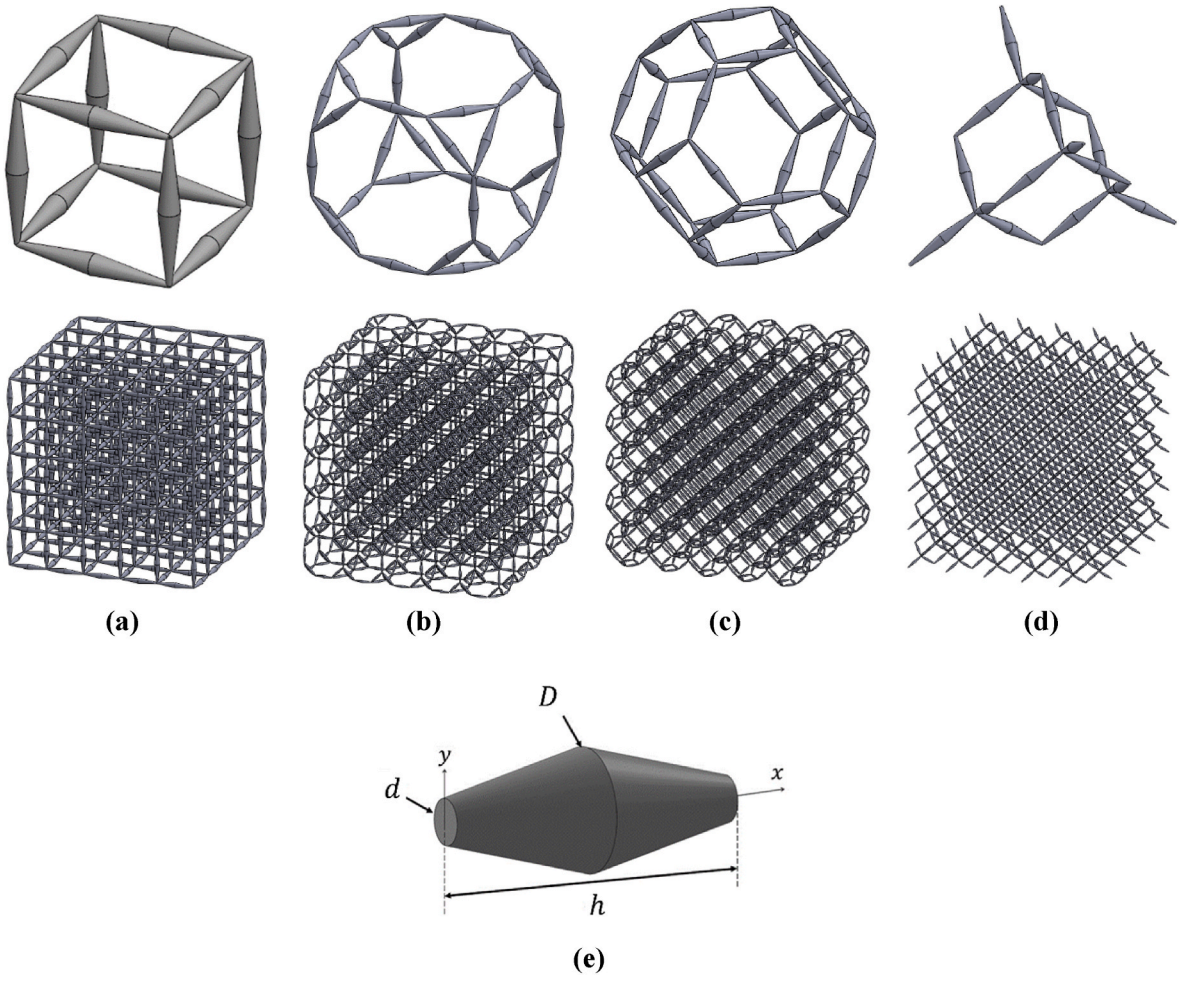


**Fig. 1.** The unit cells and corresponding lattice structures considered for this study: (a) cube, (b) truncated cube, (c) truncated octahedron, and (d) diamond topologies. (e) The dimensions of struts.

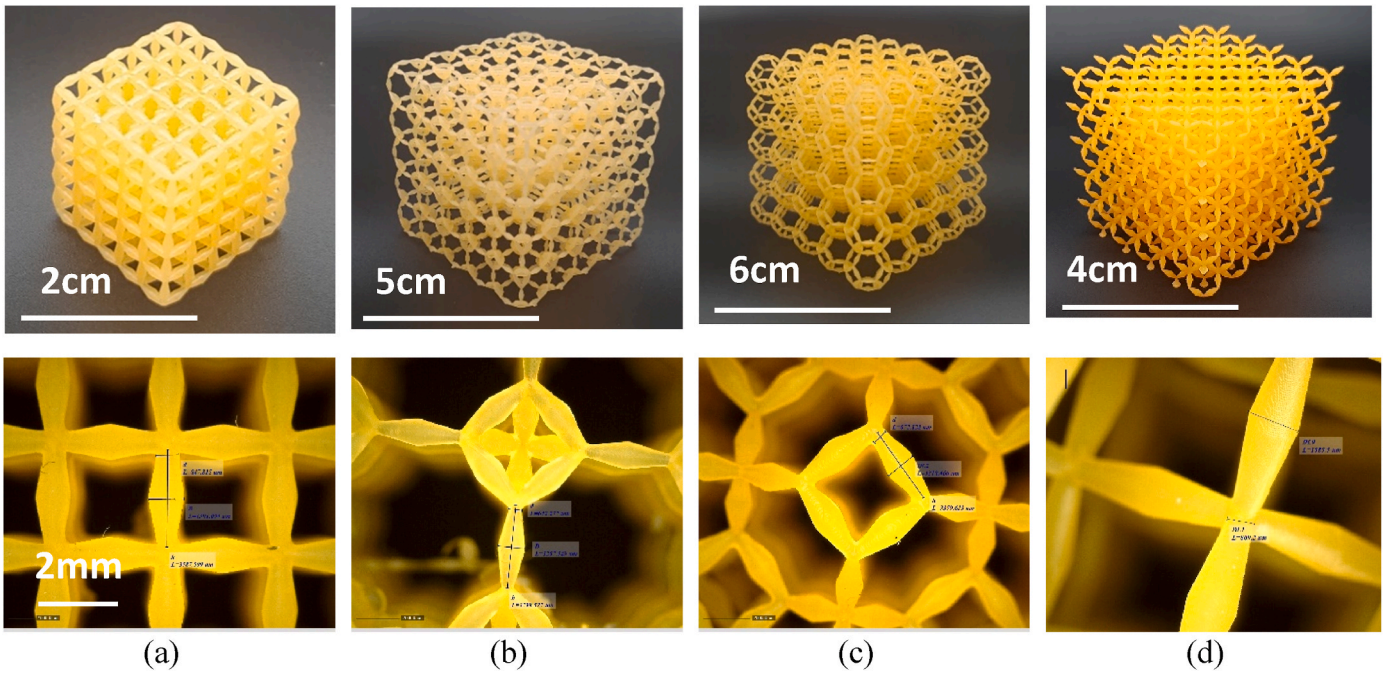


**Fig. 2.** The macroscopic and microscopic images of the manufactured pentamodes based on (a) cube, (b) truncated cube, (c) truncated octahedron, and (d) diamond topologies.

**Table 1**
Geometrical parameters of all topologies.

| $h$ (mm) | $d$ ($\mu m$) | $h/d$ | $\alpha = D/d$ |
|---|---|---|---|
| 12 | 200 | 60 | 1, 2, 3, 4, 5 |
| | 400 | 30 | 1, 2, 3, 4, 5 |
| | 600 | 20 | 1, 2, 3, 4, 5 |
| | 800 | 15 | 1, 2, 3, 4, 5 |
| | 1000 | 12 | 1, 2, 3, 4, 5 |

vertical direction. To obtain the elastic modulus, the elastic energy absorbed in the structure was measured, and inserted in the relationship $E = 2UL/A\delta^2$, where $U$, $L$, $A$, and $\delta$ denote the strain energy, dimension of the lattice structure parallel to the loading direction, structure's cross-sectional area perpendicular to the loading direction, and the resulting displacement. Similar simulations were carried out for obtaining the shear modulus, where the lattice structure top surface was moved parallel to its plane. In the models constructed for hydrostatic compressive loading, in each cartesian direction, one face of the lattice structure was constrained, and the other face was displaced uniformly. The bulk modulus was obtained from the elastic energy: $B = 2U/9L\delta^2$. The shear modulus was obtained from $G = 2UL/A\delta^2$. Mesh sensitivity analyses were performed, and it was found that element sizes in the range of 14–110 $\mu m$ gives acceptable results.

## 3. Results and discussions

The discrepancies between the elastic modulus obtained from the numerical models and experimental tests were less than 9.5%, 21.5%, and 15.5% for the cubic, truncated cube, and truncated octahedron structures, respectively. The observed discrepancies between the experimental and numerical results can be attributed to surface imperfections inherent in the fabricated samples. The presence of microcracks on the surface disrupts the material's homogeneity, leading to a reduction in its mechanical properties. Furthermore, the layered fabrication of the piece introduces additional inhomogeneity, contributing to the observed deviations. The elastic modulus obtained for the cube structure was one order of magnitude greater than the corresponding values in other geometries. In general, increasing the smaller diameter $d$ increased the elastic modulus in all the geometries exponentially (Fig. S2). The exponential effect of increasing $d$ on the elastic modulus was more significant in the diamond structure compared to other geometries. The relative elastic modulus for small diameter of $d = 400\ \mu m$ and for $\alpha = 5$ was $3.9 \times 10^{-6}$, $5.27 \times 10^{-4}$, $6.7 \times 10^{-3}$, and $2.56 \times 10^{-6}$ for the truncated octahedron, truncated cube, cube, and diamond lattice structures, respectively (Fig. S2). The effect of $\alpha$ on the increase in the elastic modulus was almost linear for the cubic structure, while its effect on other topologies was exponential (Fig. S2). As expected, in all structures, the highest strain and stress levels occurred at the tip of double-cones (Fig. 3). A relatively high level of similarity between the stress and displacement contours in different struts of the lattice structure could be observed in the bending-dominated structures, i.e. the diamond structure where all struts are inclined and to some degree in the truncated octahedron structure where a high percentage of struts are inclined. This is due to more homogeneous distribution of the applied external load in all the struts when the arrangement of the struts is similar throughout the whole structure.

Increasing the smaller diameter had a monotonic decreasing effect on the Poisson's ratio of the truncated octahedron, while it had negligible effect on the Poisson's ratio of the truncated cube and diamond structures, and it had a non-monotonic effect on the cubic structure (Fig. S3). For all the ranges of $d$ and $\alpha$, the Poisson's ratio of the truncated octahedron, truncated cube, cube, and diamond lattice structures were in the range of $0.49 - 0.57$, $0.15 - 0.22$, $0.04 - 0.4$, and $0.48 - 0.62$, respectively (Fig. S3). Increasing the $\alpha$ value had a negligible effect on the Poisson's ratio of the truncated octahedron and diamond structures, while its effect on the cube structure was non-monotonic (Fig. S3). Increasing the $\alpha$ value changed the Poisson's ratio of the truncated cube structure only for very large $d$ and $\alpha$ values (Fig. S3d).

Increasing the smaller diameter $d$ had a monotonic increasing effect on the yield stress of the truncated cube and diamond structures (Fig. S4). In the truncated octahedron and cube topologies, on the other hand, the exponential growth diminished at $d = 1000\ \mu m$ (Fig. S3). The relative yield stress for the small diameter of $d = 400\ \mu m$ and for $\alpha = 5$ was $1.1 \times 10^{-6}$, $8.16 \times 10^{-5}$, $1.1 \times 10^{-3}$, and $2.98 \times 10^{-8}$ for the

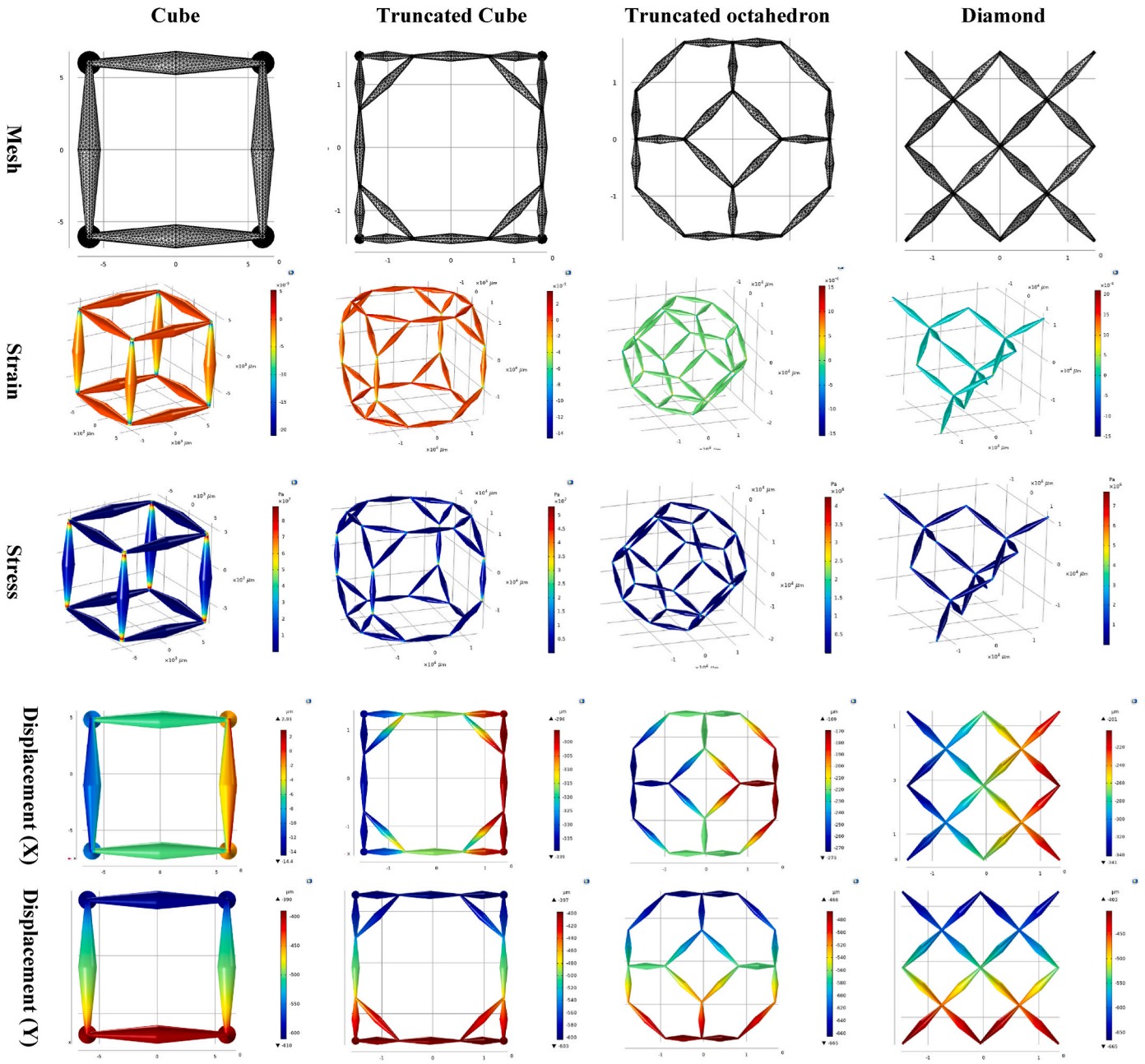


**Fig. 3.** The discretization, strain contours, stress contours, and displacement contours for pentamodes based on cube, truncated cube, truncated octahedon, and diamond topologies ($d = 400\,\mu m$ and $\alpha = 4$).

truncated octahedron, truncated cube, cube, and diamond lattice structures, respectively (Fig. S4). Therefore, the yield strength of the cubic structure was three orders of magnitude greater than that of the truncated cuboctahedron and five orders of magnitude greater than that of diamond structure. Increasing the $\alpha$ ratio had a more or less increasing effect on the yield stress of all the structures other than truncated octahedron (Fig. S4). In the truncated octahedron topology, the $\sigma_y - \alpha$ curve could get a bell-shaped geometry (Fig. S4b).

Increasing the smaller diameter $d$ had a monotonic decreasing effect on the $B/G$ ratio of the truncated octahedron and diamond structures (Fig. 4). The $B/G$ ratio in the truncated cube topology had a peak at $d = 400\,\mu m$ for $\alpha = 5$ and $\alpha = 4$ (Fig. 4). The $B/G$ ratio for the small diameter of $d = 400\,\mu m$ and for $\alpha = 5$ was 456, 575, 640, and 600 for the truncated octahedron, truncated cube, cube, and diamond lattice structures, respectively (Fig. 4). The greatest measured $B/G$ ratio for the truncated octahedron, truncated cube, cube, and diamond lattice structures was 835, 1273, 3092, and 1880, respectively. This shows that the cubic structure had the greatest $B/G$ ratio, while the truncated octahedron demonstrated the smallest $B/G$ ratio. After the cubic structure, the greatest $B/G$ ratio belonged to the diamond structure.

Independence of $B/G$ from $\alpha$ ratio has always been an important characteristic of pentamode metamaterials. Hence, studying the effect of $\alpha$ on $B/G$ in topologies other than diamond is very important. The results show that the B/G ratio of pentamode based on diamond unit cell is almost independent of $\alpha$ for $d = 400 - 1000\,\mu m$ (Fig. 4h). Some small differences in the curve of $B/G$ vs. $\alpha$ can be observed for the diamond structure with $d = 200\,\mu m$ (Fig. 4h). Interestingly, the $B/G$ ratio of the truncated octahedron and cube topologies are independent from $\alpha$ for all small diameter levels (Fig. 4b–f). The truncated cube structure is the only structure that shows some dependencies on the $\alpha$ ratio, although it is relatively small for $d \geq 600\,\mu m$.

Comparing all the $B/G$ ratios at all ranges of $\alpha$ and small diameters $d$,

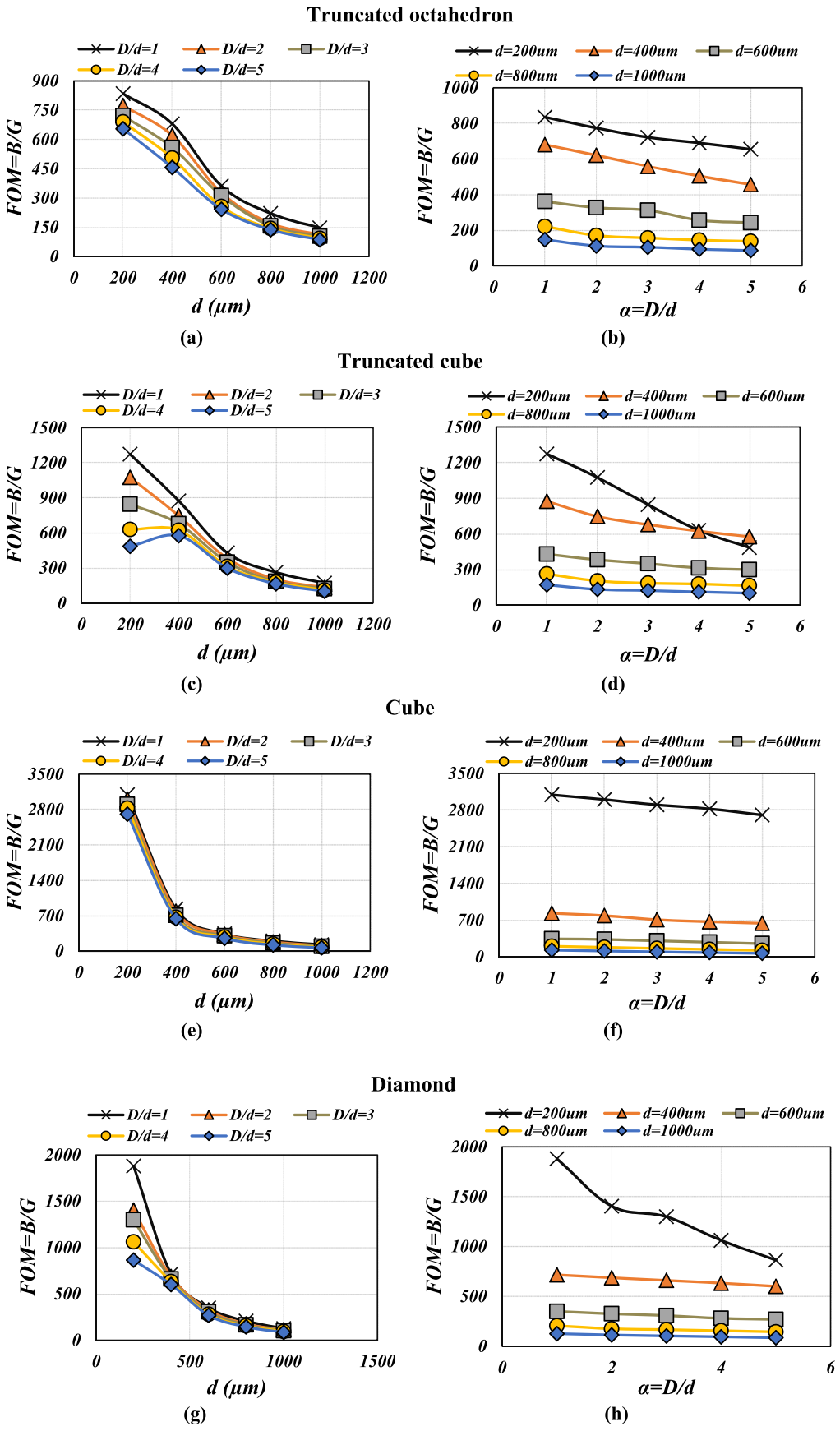


**Fig. 4.** Effect of variation of the connection point diameter ***d*** (left column) and ***α*** (right column) on the ratio of bulk modulus to shear modulus for pentamodes based on (a–b) truncated octahedon, (c–d) truncated cube, (e–f) cube, and (g–h) diamond topologies.

in small $d$, i.e. $d = 200\ \mu m$, the cubic structure has a very high $B/G$ ratio in the range of $3 \times 10^3$, while the truncated octahedron unit cell has the smallest $B/G$ ratio (Fig. 5). In large $d$, i.e. $d = 1000\ \mu m$, the truncated cube structure has the highest $B/G$ ratio (around 120), while the cubic unit cell has the smallest $B/G$ ratio (Fig. 5).

Looking at the results obtained, it can be seen that, the $B/G$ ratio is almost independent from the $\alpha$ value, especially for structures with $\frac{d}{h} > 0.05$. This is because after exerting an external load, the stress is mostly concentrated at the touching points of the double-cones, and the other parts do not significantly influence the load-bearing capacity of the structure. Therefore, by varying the size of the thick part, one can adjust the density of the lattice structure without changing its mechanical response over a large range [17]. This can lead to structures with decoupled modulus and relative density, in contrast to other porous materials [23–27] which show a strong correlation between their density and mechanical properties [24,28,29]. Such a property can be very appealing in designing biomedical implants where it is desired to have independent distributions of mechanical properties and permeability [20,30].

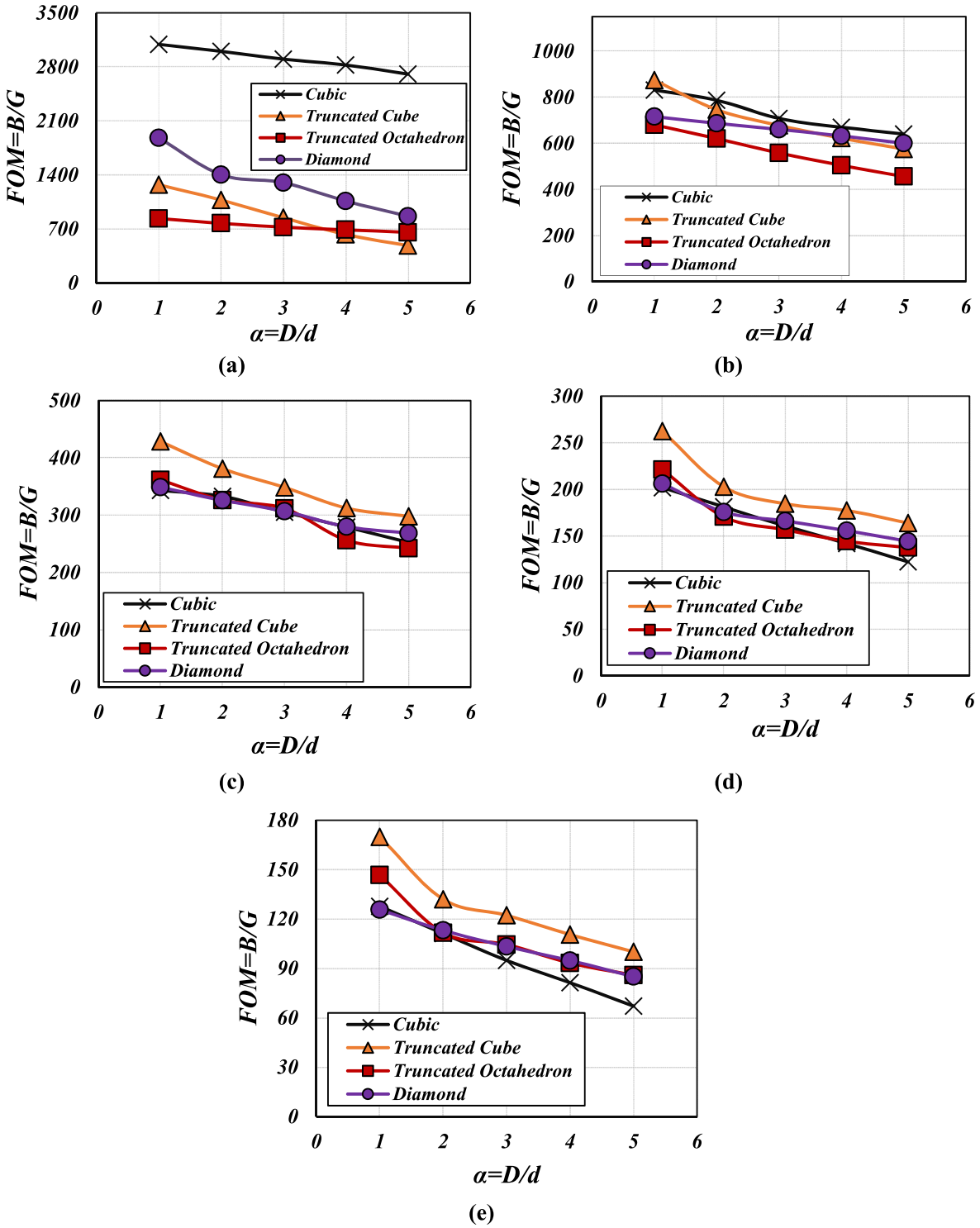


**Fig. 5.** Effect of variation of $\alpha$ on the ratio of bulk modulus to shear modulus for smaller diameters of (a) **200** $\mu m$ , (b) $\mu m$, (c) **00** $\mu m$, (d) **800** $\mu m$, and (e) **1000** $\mu m$.

## 4. Conclusions

In summary, the mechanical properties of four types of lattice structures (cube, truncated cube, diamond, and truncated octahedron) with double-cone struts were studied experimentally and numerically, and the effect of sizes of the smaller $d$ and larger $D$ diameters of the double-cones on the figure of merit (FOM), i.e. the $B/G$ ratio, was studied. It was observed that regardless of the base unit cell shape, the FOM value is highly dependent on the tip diameter $d$ value, but its dependence on the thicker part with $D$ value is very weak. For $d/h \propto 0.05$ ($h$ representing the linkage length), FOMs in the range of $10^3$ could be reached for all the topologies considered.

## CRediT authorship contribution statement

**Kaivan Mohammadi:** Data curation, Formal analysis, Investigation, Methodology, Software, Supervision, Validation, Writing – original draft. **Moein Shafia:** Investigation, Methodology, Software, Visualization, Writing – original draft. **Javad Akbari:** Conceptualization, Formal analysis, Investigation, Methodology, Software, Supervision, Writing – original draft. **Reza Hedayati:** Conceptualization, Data curation, Investigation, Methodology, Software, Supervision, Validation, Visualization, Writing – original draft, Writing – review & editing.

## Declaration of competing interest

The authors declare that they have no known competing financial interests or personal relationships that could have appeared to influence the work reported in this paper.

## Data availability

Data will be made available on request.

## Appendix A. Supplementary data

Supplementary data to this article can be found online at https://doi.org/10.1016/j.rineng.2024.101982.

## References

[1] W. Wu, W. Hu, G. Qian, H. Liao, X. Xu, F. Berto, Mechanical design and multifunctional applications of chiral mechanical metamaterials: a review, Materials & design 180 (2019) 107950.
[2] E. Barchiesi, M. Spagnuolo, L. Placidi, Mechanical metamaterials: a state of the art. Mathematics and Mechanics of Solids 24 (1) (2019) 212–234.
[3] A. Zhao, X. Zhang, W. Yu, Z. Zhao, X. Cai, H. Chen, Design and simulation of broadband multiphase pentamode metamaterials, Appl. Phys. Lett. 118 (22) (2021) 224103.
[4] D.H. Helmy, H. El Arabaty, M. Nour, L. Placidi, M.G. El Sherbiny, Evaluation of the seismic response of frames implemented with metamaterials, Results in Engineering 18 (2023) 101197.
[5] K. Mizukami, R. Imanishi, H. Matsushita, Y. Koga, Design and additive manufacturing of elastic metamaterials with 3D lever-type inertial amplification mechanisms for mitigation of low-frequency vibration, Results in Engineering 20 (2023) 101389.
[6] R. Hedayati, A. Güven, S. Van Der Zwaag, 3D gradient auxetic soft mechanical metamaterials fabricated by additive manufacturing, Appl. Phys. Lett. 118 (14) (2021) 141904.
[7] L. Yang, O. Harrysson, H. West, D. Cormier, Mechanical properties of 3D re-entrant honeycomb auxetic structures realized via additive manufacturing. International Journal of Solids and Structures 69 (2015) 475–490.
[8] R. Hedayati, N. Roudbarian, S. Tahmasiyan, M. Bodaghi, Gradient origami metamaterials for programming out-of-plane curvatures, Adv. Eng. Mater. 25 (14) (2023) 2201838.
[9] T.A. Hewage, K.L. Alderson, A. Alderson, F. Scarpa, Double-negative mechanical metamaterials displaying simultaneous negative stiffness and negative Poisson's ratio properties. Advanced materials 28 (46) (2016) 10323–10332.
[10] Y. Sun, N.M. Pugno, In plane stiffness of multifunctional hierarchical honeycombs with negative Poisson's ratio sub-structures, Compos. Struct. 106 (2013) 681–689.
[11] K. Mohammadi, M. Movahhedy, I. Shishkovsky, R. Hedayati, Hybrid anisotropic pentamode mechanical metamaterial produced by additive manufacturing technique, Appl. Phys. Lett. 117 (6) (2020) 61901.
[12] A. Krushynska, P. Galich, F. Bosia, N. Pugno, S. Rudykh, Hybrid metamaterials combining pentamode lattices and phononic plates, Appl. Phys. Lett. 113 (20) (2018) 201901.
[13] A. Martin, M. Kadic, R. Schittny, T. Bückmann, M. Wegener, Phonon band structures of three-dimensional pentamode metamaterials, Phys. Rev. B 86 (15) (2012) 155116.
[14] T. Bückmann, M. Kadic, R. Schittny, M. Wegener, Mechanical cloak design by direct lattice transformation, Proc. Natl. Acad. Sci. USA 112 (16) (2015) 4930–4934.
[15] G.W. Milton, A.V. Cherkaev, Which elasticity tensors are realizable? J. Eng. Mater. Technol. 117 (4) (1995) 483–493.
[16] R. Schittny, T. Bückmann, M. Kadic, M. Wegener, Elastic measurements on macroscopic three-dimensional pentamode metamaterials, Appl. Phys. Lett. 103 (23) (2013) 231905.
[17] M. Kadic, T. Bückmann, R. Schittny, P. Gumbsch, M. Wegener, Pentamode metamaterials with independently tailored bulk modulus and mass density, Phys. Rev. Appl. 2 (5) (2014) 54007.
[18] Y. Huang, X. Lu, G. Liang, Z. Xu, Pentamodal property and acoustic band gaps of pentamode metamaterials with different cross-section shapes, Phys. Lett. 380 (13) (2016) 1334–1338.
[19] M. Kadic, T. Bückmann, N. Stenger, M. Thiel, M. Wegener, On the practicability of pentamode mechanical metamaterials, Appl. Phys. Lett. 100 (19) (2012) 191901.
[20] R. Hedayati, A. Leeflang, A. Zadpoor, Additively manufactured metallic pentamode meta-materials, Appl. Phys. Lett. 110 (9) (2017) 91905.
[21] H. Fallahi, M. Sadighi, S.S. Samandari, Compressive mechanical properties of open-cell cubic and rhombic dodecahedron lattice structures of variable cross section fabricated by fused deposition modeling, Mech. Mater. (2023) 104712.
[22] G. Rico-Baeza, E. Cuan-Urquizo, G.I. Pérez-Soto, L.A. Alcaraz-Caracheo, K. A. Camarillo-Gómez, Additively manufactured lattice materials with a double level of gradation: a comparison of their compressive properties when fabricated with material extrusion and vat photopolymerization processes, Materials 16 (2) (2023) 649.
[23] N. Ghavidelnia, R. Hedayati, M. Sadighi, M. Mohammadi-Aghdam, Development of porous implants with non-uniform mechanical properties distribution based on CT images, Appl. Math. Model. 83 (2020) 801–823.
[24] R. Hedayati, N. Ghavidelnia, M. Sadighi, M. Bodaghi, Improving the accuracy of analytical relationships for mechanical properties of permeable metamaterials, Appl. Sci. 11 (3) (2021) 1332.
[25] C.N. Kelly, A.T. Miller, S.J. Hollister, R.E. Guldberg, K. Gall, Design and structure–function characterization of 3D printed synthetic porous biomaterials for tissue engineering, Adv. Healthcare Mater. 7 (7) (2018) 1701095.
[26] A. Alaimo, A. Del Prete, G. Mantegna, et al., Modified beam modeling of powder bed fusion manufactured lattice structures, Int. J. Mech. Sci. 259 (2023) 108599.
[27] D. Tumino, A. Alaimo, G. Mantegna, C. Orlando, S. Valvano, Mechanical properties of BCC lattice cells with waved struts, Int. J. Interact. Des. Manuf. (2023) 1–14.
[28] X. Zheng, H. Lee, T.H. Weisgraber, et al., Ultralight, ultrastiff mechanical metamaterials. Science 344 (6190) (2014) 1373–1377.
[29] M.F. Ashby, D. Cebon, Materials selection in mechanical design, J. Phys. IV (1993) 3. C7): p. C7-1-C7-9.
[30] A.A. Zadpoor, Mechanical meta-materials, Mater. Horiz. 3 (2016) 371–381.